

## Transmission Characteristics of Long-Period Fiber Gratings Using Periodically Corroded Single-Mode Fibers

Jonghwan Lee<sup>1</sup>, Ngac An Bang<sup>2</sup>, and Young-Geun Han<sup>3\*</sup>

<sup>1</sup>*School of Industrial Engineering, Kumoh National Institute of Technology, Gumi 730-701, Korea*

<sup>2</sup>*Vietnam National University-University of Science, Hanoi, Vietnam*

<sup>3</sup>*Department of Physics and Research Institute for Convergence of Basic Science, Hanyang University, Seoul 133-791, Korea*

(Received March 25, 2015 : revised June 1, 2015 : accepted June 26, 2015)

Transmission characteristics of long-period fiber gratings (LPFGs) fabricated by periodically etching a conventional single-mode fiber (SMF) are investigated. After coating the SMF with photoresist, the cladding of the SMF is symmetrically and periodically removed by using a wet etching technique resulting in the formation of the LPFG. Tensile strain reinforces the coupling strength between the core and the cladding mode based on the photoelastic effect. The extinction ratio of the SMF-based LPFG at a wavelength of 1550.8 nm is measured to be -15.1 dB when the applied strain is 600  $\mu\epsilon$ . The ascent of ambient index shifts the resonant wavelength to shorter wavelength because of the increase of the effective refractive index of the cladding mode. The extinction ratio is diminished by increase in the ambient index because of the induction of the optical attenuation of the cladding mode. The transmission characteristics of the proposed LPFG with variations in torsion are also measured. The photoelastic effect based on torsion changes the extinction ratio and the resonant wavelength of the proposed SMF-based LPFG. The polarization-dependent loss of the LPFG is also increased by torsion because of the torsion-induced birefringence. The polarization-dependent loss of the LPFG at torsion of 8.5 rad/m is measured to be 3.9 dB.

*Keywords* : Long-period fiber gratings, Fiber-optic sensors, Photoelastic effect

*OCIS codes* : (060.0060) Fiber optics and optical communications; (060.2370) Fiber optics sensors; (050.2770) Gratings

### I. INTRODUCTION

Fiber gratings, such as fiber Bragg gratings and long-period fiber gratings (LPFGs), have been significantly advanced in optical communication systems and optical sensors because of their many advantages, such as wavelength-selective nature, high tunability, electromagnetic immunity, etc. [1-5] LPFGs can basically couple a fundamental core mode to the forward propagating cladding modes resulting in harmonic resonant peaks in the transmission spectrum. Cladding modes play an important role in realizing fiber-optic sensors based on LPFGs with high sensitivity to external perturbation change, such as temperature and strain [1-3]. There is much research on the development of fabrication techniques of LPFGs [6-19]. A conventional LPFG can be simply fabricated by exposing single-mode fibers (SMFs) with a germanium-doped

core to UV excimer lasers and frequency-doubled argon lasers [1]. For specialty fibers without photosensitivity, such as photonic crystal fibers (PCFs), different fabrication techniques are required to generate the periodic index modulation for the realization of LPFGs [2, 6-19]. The etching method to induce the periodic deformation of the silica cladding in the dispersion-shifted fiber (DSF) was proposed by using a hydrofluoric acid (HF) solution incorporating the metal coating procedure [16]. However, it is not easy to make symmetrical and periodic metal coating layers on the cylindrical cladding of the DSF. Recently, two fabrication techniques of LPFGs including a thick photoresist and an inductively coupled plasma technique were proposed [17, 18]. In the previous two methods, however, a sacrificial copper layer was first coated on the wafer resulting in the induction of additional loss. It is not evident if the two previous methods are capable of deeply

\*Corresponding author: [yghan@hanyang.ac.kr](mailto:yghan@hanyang.ac.kr)

Color versions of one or more of the figures in this paper are available online.

corroding the silica cladding of an optical fiber because the reduction of the cladding diameter of the optical fiber was preprocessed. This means that the previous methods cannot readily fabricate the LPFG using a conventional SMF with lower photoelastic effect than the DSF. The periodic polymer patterns still remained in the surface of the LPG after etching the silica cladding [17]. The inductively coupled plasma (ICP) method may not be capable of deeply etching the silica cladding of the optical fiber [18]. Therefore, it is still necessary to consider a fabrication technique of LPFGs based on the regular SMFs with a low photoelastic coefficient.

In this work, we discuss transmission characteristics of LPFGs fabricated by periodically etching a conventional SMF. The silica cladding of the regular SMF is periodically removed by using a wet etching technique incorporating the double-layered photoresist coating overlay. The periodic deformation in the cladding of the SMF induces the periodic index modulation based on the photoelastic effect when tensile strain is applied and consequently generates the resonant peak wavelengths in the transmission spectrum resulting from the mode coupling between the core and cladding modes in the LPFG. The effects of ambient index and torsion on the resonant wavelength and the extinction ratio of the proposed LPFG are presented. The torsion-induced birefringence changes polarization-dependent loss (PDL) of the proposed LPFG.

## II. FABRICATION OF THE SMF-BASED LPFG

Figure 1(a) indicates the structure of the proposed LPFG with periodic micro-ridges in the cladding region of the conventional SMF. It is important to symmetrically remove the silica cladding of the SMF because of its cylindrical structure. Photoresist with a thickness of  $150\ \mu\text{m}$  was

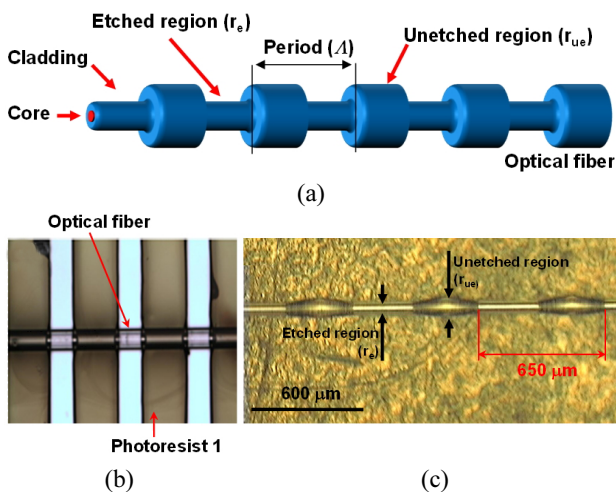


FIG. 1. (a) Structure of the proposed LPFG based on the SMF, (b) photograph of the SMF with symmetrical and periodic photoresist patterns after the developing process, and (c) photograph of the fabricated LPFG based on the SMF measured using an optical microscope

spin-coated on the substrate. Then we put a conventional SMF on the substrate with photoresist and recoated it with the same photoresist with a thickness of  $150\ \mu\text{m}$ . The prebaking process was taken to remove the solvent in photoresist. To remove photoresist periodically, we exposed the SMF with photoresist to a UV lamp through an amplitude mask. The length and the period of the amplitude mask were  $20\ \text{mm}$  and  $650\ \mu\text{m}$ , respectively. Since photoresist exposed to a UV light is readily eliminated by using a developer, the symmetric and periodic photoresist pattern was imprinted on the surface of the SMF. Figure 2(b) shows the photograph of the SMF with symmetrical and periodic photoresist patterns after the developing process. The SMF with the periodic and symmetric photoresist patterns was immersed in the hydrofluoric acid solution to remove the silica cladding that was not covered with photoresist, which results in the reduction of the diameter of the SMF. Since the periodic photoresist patterns effectively prevent the silica cladding of the SMF from being corroded by the hydrofluoric acid solution, the diameter of the SMF with photoresist patterns should be less reduced than that without photo-

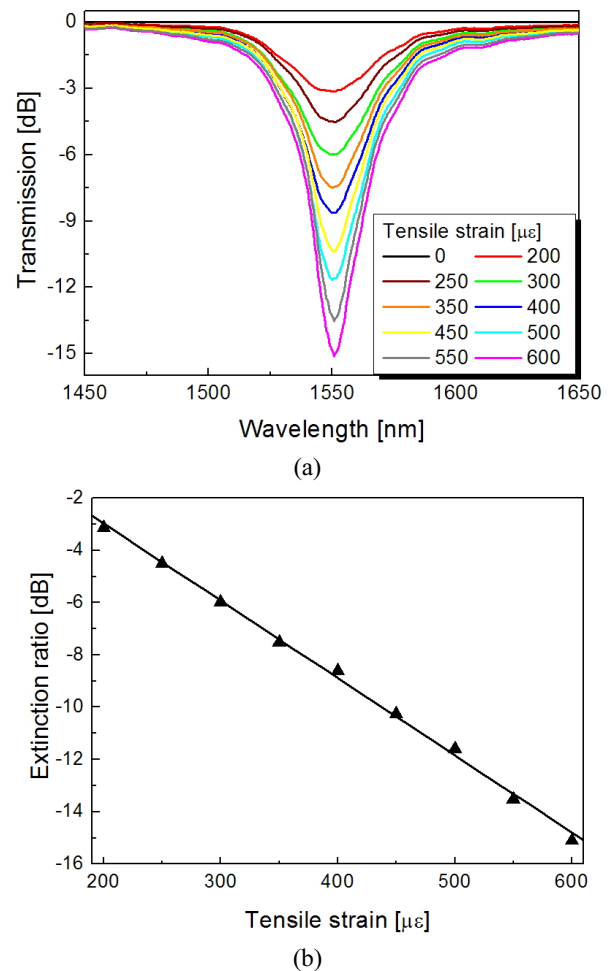


FIG. 2. (a) Transmission spectra with variations in strain and (b) variation of the extinction ratio as a function of the applied strain.

resist patterns. The periodic and symmetric micro-ridges on the surface of the SMF were finally achieved. Figure 2(c) shows the photograph of the fabricated LPFG based on the SMF measured by using an optical microscope. The grating period ( $\Lambda$ ) of the LPFG was measured to be 650  $\mu\text{m}$ , which was determined by that of the amplitude mask during the developing procedure. The periodic index modulation in the SMF can be induced by applying tensile strain because of the different photoelastic effect in the etched and the unetched cladding regions with distinct cladding diameters. Therefore, we successfully realized the SMF-based LPFG by symmetrically engraving the periodic corrugation patterns on the surface of the SMF.

### III. RESULTS AND DISCUSSION

Since the etched and the unetched regions in Fig. 1(a) have different radii,  $r_e$  and  $r_{ue}$ , respectively, the applied force induces the distinct variations of refractive indices based on the photoelastic effect in two regions ( $\delta n_e(r)$  and  $\delta n_{ue}(r)$  in the etched and the unetched regions, respectively), which can be written as [16, 19]

$$\delta n_e(r) = -\frac{1}{2} p [n_e^{(0)}(r)]^3 \frac{F}{Y \pi r_e^2}, \text{ in the etched region} \quad (1)$$

$$\delta n_{ue}(r) = -\frac{1}{2} p [n_{ue}^{(0)}(r)]^3 \frac{F}{Y \pi r_{ue}^2}, \text{ in the unetched region} \quad (2)$$

where  $p$  is the effective photoelastic coefficient related with the Poisson's ratio.  $Y$  is the Young's modulus.  $F$  is the applied force.  $n_e^{(0)}(r)$  and  $n_{ue}^{(0)}(r)$  are the unperturbed index profiles of the etched and the unetched regions, respectively. Since the unperturbed index profiles before applying the external force are almost the same, the periodic variation ( $\Delta n_f$ ) of the refractive index due to the external force ( $F$ ) can be derived as [16, 19].

$$\Delta n_f = \delta n_e - \delta n_{ue} = -\frac{1}{2} p [n_e^{(0)}(r)]^3 \left[ 1 - \frac{r_{ue}^2}{r_e^2} \right] F. \quad (3)$$

It is evident that the value of  $\Delta n_f$  is critically affected by the diameters of two regions. By substituting Eq. (3) to the phase matching condition of the LPFG, the strain sensitivity ( $d\lambda_p/d\varepsilon$ ) of the proposed SMF-based LPFG can be expressed by

$$\frac{d\lambda_p}{d\varepsilon} \cong -\frac{1}{2} \Lambda \left( \left[ \frac{r_u^2}{r_e^2} - 1 \right] \right) \left( p_e^{co} [n_{co}^{(0)}(r)]^3 - p_e^{cl} [n_{cl}^{(0)}(r)]^3 \right) + \frac{d\lambda_p}{d\Lambda} \frac{d\Lambda}{d\varepsilon}. \quad (4)$$

It is obvious that the negative contribution of the photo-

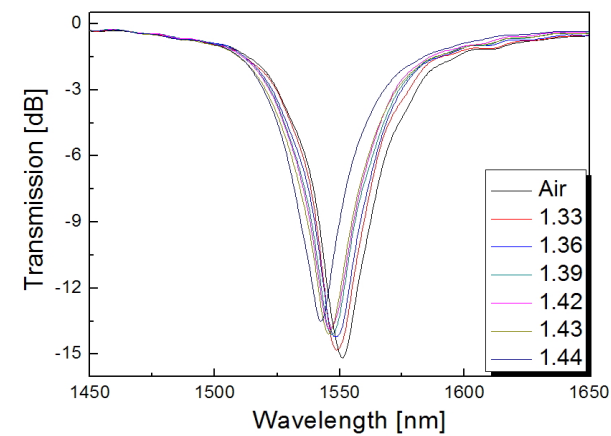
elastic effect to the strain-dependence of the resonant wavelength of the LPFG compensates the positive waveguide dispersion term in Eq. (4). Consequently, the resonant wavelength shift of the proposed LPFG with variations in strain can be negligible. Compared to the strain sensitivity of the LPFG with periodic micro-ridges, the variation of the waveguide dispersion with respect to torsion change is negligible and the torsion sensitivity of the LPFG ( $d\lambda_p/d\xi$ ) can be written as

$$\frac{d\lambda_p}{d\xi} \cong -\frac{1}{2} \Lambda \left( \left[ \frac{r_u^2}{r_e^2} - 1 \right] \right) \left( p_{e,tor}^{co} [n_{co}^{(0)}(r)]^3 - p_{e,tor}^{cl} [n_{cl}^{(0)}(r)]^3 \right). \quad (5)$$

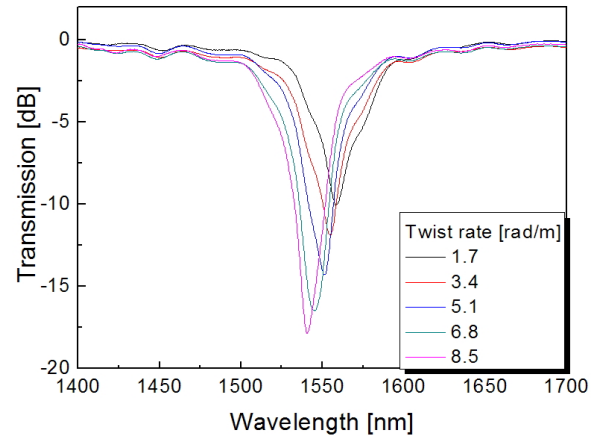
Therefore, the resonant wavelength of the LPFG with periodic micro-ridges shifts to shorter wavelength as the applied torsion increases. Figure 2(a) depicts the transmission characteristics of the proposed SMF-based LPFG with variations in strain. The mode coupling between core and cladding mode based on the photoelastic effect is gradually induced by increasing strain resulting in the enhancement of the extinction ratio at a resonant wavelength. Figure 2(b) exhibits the variation of the extinction ratio as a function of the applied strain. The variation of the extinction ratio at a wavelength of 1550.8 nm was measured to be -15.1 dB when the applied strain was 600  $\mu\epsilon$ . However, the resonant wavelength of the LPFG was not changed severely by the applied strain because of the simultaneous induction of the photoelastic effect in the core and the cladding regions. Since the applied strain identically changes the effective refractive indices of the core and the cladding modes, the positive waveguide dispersion factor will be compensated by the negative photoelastic effect induced by strain. Therefore, the resonant wavelength shift of the proposed LPFG with variations in strain is rarely observed as the mode coupling between the core and the cladding mode occurs. It is manifest that it is possible to monitor the external strain change by detecting the extinction ratio of the proposed LPFG with variations in strain.

Figure 3(a) and 3(b) indicate the transmission spectra and the resonant wavelength shift of the proposed SMF-based LPFG, respectively, with variations in ambient index. Since the effective index of the cladding mode is increased by ambient index, the resonant wavelength of the LPFG must be shifted to shorter wavelength as ambient index increases. The extinction ratio of the LPFG was degraded by ambient index because of the induction of the optical attenuation of the cladding mode. The ambient index sensitivity of the proposed SMF-based LPFG was measured to be -58.2 nm/RIU (RIU: refractive index unit).

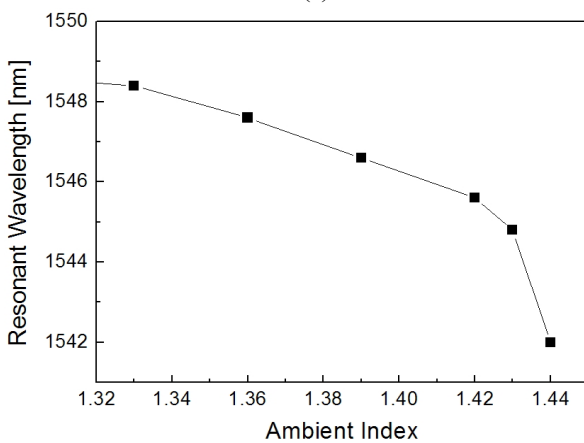
Figure 4(a) shows the transmission spectra of the proposed LPFG with variations in torsion. Since the torsion-induced photoelastic effect reinforces the coupling strength between the core and the cladding mode in the proposed LPFG, the extinction ratio should be enhanced by increasing torsion. Since the refractive index variation based on the torsion-



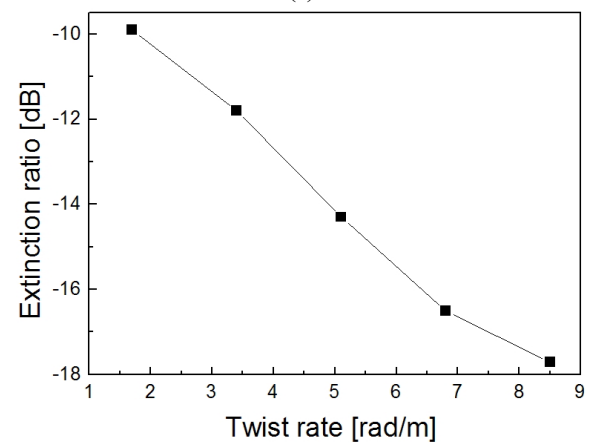
(a)



(a)



(b)

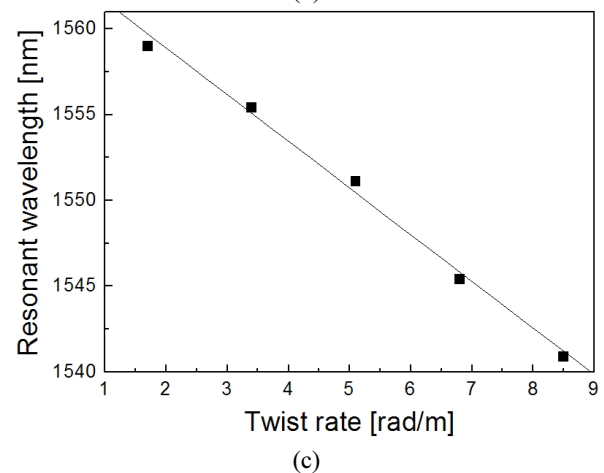


(b)

FIG. 3. (a) Transmission spectra with variations in ambient index and (b) resonant wavelength shift as a function of ambient index.

induced photoelastic effect is much higher than that based on the tensile strain-induced one and the torsion sensitivity of the LPFG is negative, the resonant wavelength shift of the LPFG with variations in torsion is apparently observed in the transmission spectra [20]. As seen in Fig. 4(b), the resonant wavelength of the LPFG shifts to shorter wavelength as the applied torsion increases.

Figure 5 shows the variation of PDL of the proposed SMF-based LPFG with variations in torsion. The PDL is closely related with the birefringence of the optical fiber. The torsion-induced elliptical birefringence resulting from different amount of twist rate in etched and unetched cladding regions increased PDL of the LPFG as seen in Fig. 5. The PDL can be defined as the maximum variation of the transmitted power for all possible polarization states. The applied torsion to the proposed SMF-based LPFG will give rise to an elliptical birefringence within the SMF-based LPFG because the induction of shearing force and twisting strain in the SMF. Since the variation of the elliptical birefringence vector is directly proportional to the external torsion [21, 22], the effective indices of the etched and the unetched



(c)

FIG. 4. (a) Transmission spectra with variations in torsion, variation of the extinction ratio (b) and the resonant wavelength (c) as a function of torsion.

regions should be distinctly changed by the external torsion resulting in two different resonant wavelengths depending on two eigen polarization states. The amount of the PDL is predominantly determined by the wavelength spacing of two resonant wavelengths based on two orthogonal polarization states. Consequently, the induction of the elliptical birefringence

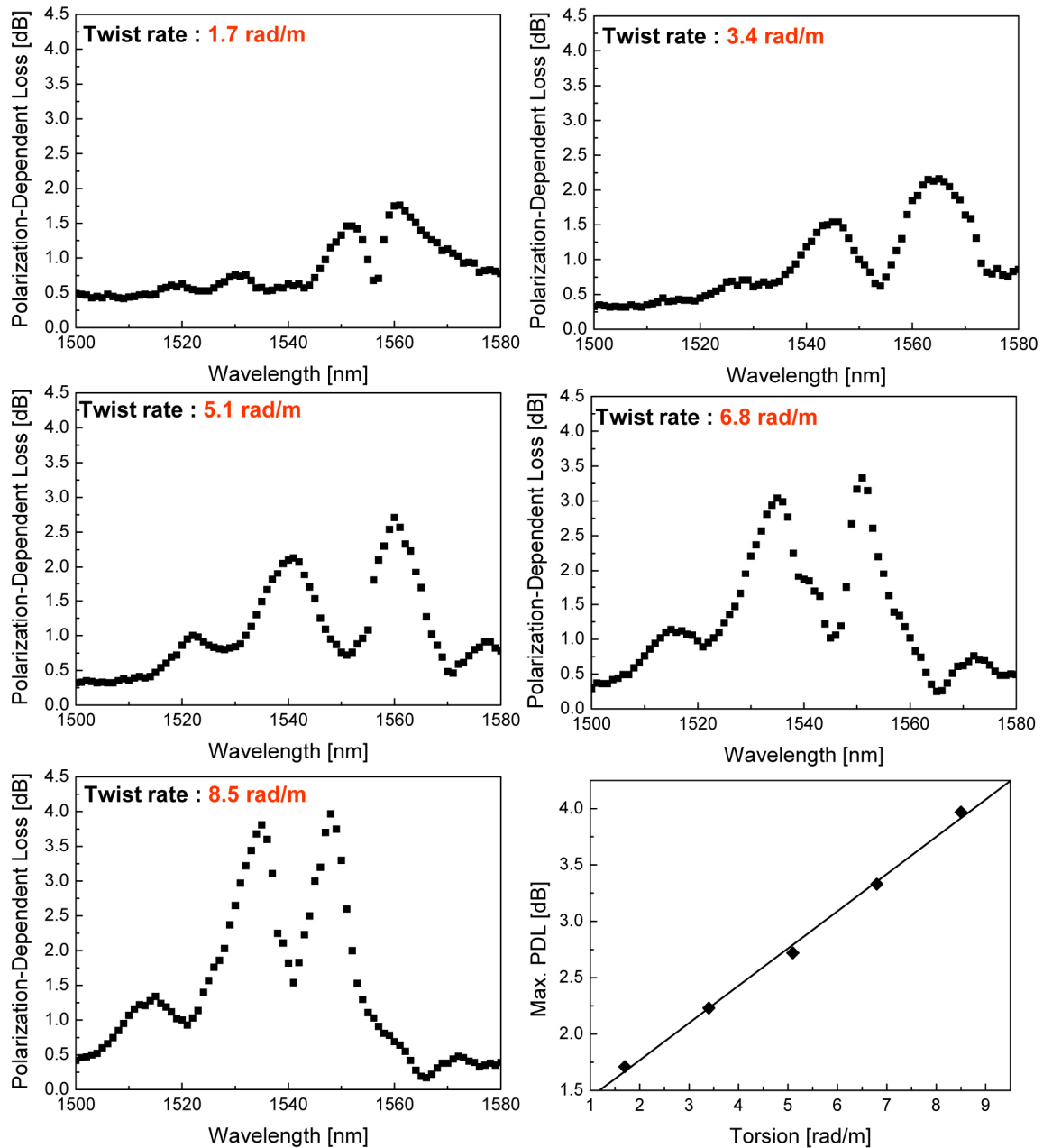


FIG. 5. Polarization-dependent loss with variations in torsion.

by the external torsion will definitely increase the amount of the PDL of the proposed SMF-based LPFG because of the torsion-induced elliptical birefringence changes the wavelength spacing of two resonant wavelengths based on two orthogonal polarization states. For a torsion of 8.5 rad/m, we measured the amount of PDL of the LPFG to be 3.9 dB.

#### IV. CONCLUSION

We discussed transmission characteristics of the LPFG manufactured by symmetrically and periodically etching a

conventional SMF. The double-layered photoresist overlay was formed in the surface of the SMF to engrave periodic and symmetrical micro-ridges on the surface of the SMF. Tensile strain applied to the SMF with periodic deformation in the cladding of the SMF successfully induced the periodic index modulation based on the photoelastic effect in the SMF. Consequently the resonant wavelengths resulting from the mode coupling between the core and the cladding mode in the SMF appeared in the transmission spectrum. The extinction ratio of the SMF-based LPFG was measured to be -15.1 at a resonant wavelength of 1550.8 nm when the applied strain was 600  $\mu\epsilon$ . The resonant wavelength of the

LPPFG was shifted to shorter wavelength by increasing ambient index because of the ascent of the effective index of the cladding mode. The extinction ratio of the LPPFG was reduced by ambient index because of the increment of the optical attenuation of the cladding mode. The photoelastic effect based on torsion shifted the resonant wavelength of the LPPFG to shorter wavelength. The polarization-dependent loss of the proposed LPPFG was increased by torsion because of the torsion-induced birefringence. The PDL of the LPPFG at a torsion of 8.5 rad/m was measured to be 3.9 dB.

### ACKNOWLEDGMENT

This paper was supported by Research Fund, Kumoh National Institute of Technology.

### REFERENCES

1. A. M. Vengsarkar, P. J. Lemaire, J. B. Judkins, V. Bhatia, T. Erdogan, and J. E. Sipe, "Long-period fiber gratings as band-rejection filters," *IEEE J. Lightwave Technol.* **14**, 58-64 (1996).
2. M. S. Yoon, H. J. Kim, S. J. Kim, and Y. G. Han, "Influence of the waist diameters on transmission characteristics and strain sensitivity of microtapered long-period fiber gratings," *Opt. Lett.* **38**, 2669-2672 (2013).
3. Z. Bai, W. Zhang, S. Gao, H. Zhang, L. Wang, and F. Liu, "Bend-insensitive long period fiber grating-based high temperature sensor," *Opt. Fiber Technol.* **21**, 110-114 (2015).
4. B. W. Kang, K. Lee, S. B. Lee, and C. Kim, "Colorless amplified WDM-PON employing broadband light source seeded optical sources and channel-by-channel dispersion compensators for >100 km Reach," *J. Opt. Soc. Korea* **18**, 436-441 (2014).
5. H. Kim and M. Song, "A fiber laser spectrometer demodulation of fiber Bragg grating sensors for measurement linearity enhancement," *J. Opt. Soc. Korea* **17**, 312-316 (2013).
6. X. Lan, Q. Han, J. Huang, H. Wang, Z. Gao, A. Kaur, and H. Xiao, "Turn-around point long-period fiber grating fabricated by CO<sub>2</sub> laser for refractive index sensing," *Sens. Actuators B: Chemical* **177**, 1149-1155 (2013).
7. Y. Jiang, C. Tang, and J. Xu, "Fabrication of long-period gratings with a mercury-arc lamp," *Opt. Commun.* **283**, 1311-1315 (2010).
8. F. Zou, Y. Liu, C. Deng, Y. Dong, S. Zhu, and T. Wang, "Refractive index sensitivity of nano-film coated long-period fiber gratings," *Opt. Express* **23**, 1114-1124 (2015).
9. P. Wang, L. Xian, and H. Li, "Fabrication of phase-shifted long-period fiber grating and its application to strain measurement," *IEEE Photon. Technol. Lett.* **27**, 557-560 (2015).
10. L. Wang, W. Zhang, F. Liua, L. Chena, Z. Cui, and T. Yan, "Mechanism and characteristics of asymmetrically phase-shifted corrugated long-period fiber grating fabricated by burning fiber coating and etching cladding technology," *J. Mod. Opt.* **62**, 584-587 (2015).
11. A. Iadicicco, S. Campopiano, and A. Cusano, "Long period gratings in hollow core fibers by pressure assisted arc discharge technique," *IEEE Photon. Technol. Lett.* **23**, 1567-1569 (2011).
12. W. Huang, Y. Liu, Z. Wang, B. Liu, J. Guo, M. Luo, and L. Lin, "Intermodal interferometer with low insertion loss and high extinction ratio composed of a slight offset point and a matching long period grating in two-mode photonic crystal fiber," *Appl. Opt.* **54**, 285-290 (2015).
13. C. Liao, Y. Wang, D. N. Wang, and L. Jin, "Femtosecond laser inscribed long-period gratings in all-solid photonic bandgap fibers," *IEEE Photon. Technol. Lett.* **22**, 425-427 (2010).
14. B. Wang, W. Zhang, Z. Bai, L. Wang, L. Zhang, Q. Zhou, L. Chen, and T. Yan, "CO<sub>2</sub>-laser-induced long period fiber gratings in few mode fibers," *IEEE Photon. Technol. Lett.* **27**, 145-1569 (2011).
15. M. Yang, D. N. Wang, Y. Wang, and C. Liao, "Long period fiber grating formed by periodically structured microholes in all-solid photonic bandgap fiber," *Opt. Express* **18**, 2183-2189 (2010).
16. C. Y. Lin and L. A. Wang, "Corrugated long-period fiber gratings as strain, torsion, and bending sensors," *IEEE J. Lightwave Technol.* **8**, 1159-1168 (2001).
17. M. S. Yoon, S. H. Park, and Y. G. Han, "Simultaneous measurement of strain and temperature by using a micro-tapered fiber grating," *IEEE J. Lightwave Technol.* **30**, 1156-1160 (2012).
18. M. Huang, "Stress effects on the performance of optical waveguides," *International Journal of Solids and Structures* **40**, 1615-1632 (2003).
19. A. Galtarossa and L. Palmieri, "Measure of twist-induced circular birefringence in long single-mode fibers: Theory and Experiments," *IEEE J. Lightwave Technol.* **20**, 1149-1159 (2002).
20. Y. J. Rao, T. Zhu, and Q. J. Mo, "Highly sensitive fiber-optic torsion sensor based on an ultra-long-period fiber grating," *Opt. Commun.* **266**, 187-190 (2006).